Józef SALWIŃSKI*, Piotr GRĄDKOWSKI*

EXPERIMENTAL VERIFICATION OF A MODEL OF THE LOSS OF FLUID FRICTION IN A HYBRID THRUST BEARING

EKSPERYMENTALNA WERYFIKACJA MODELU UTRATY TARCIA PŁYNNEGO W HYBRYDOWYM ŁOŻYSKU WZDŁUŻNYM

Key words:

thrust bearing, hydrostatic lubrication, pressure distribution measurement

Słowa kluczowe:

łożysko wzdłużne, smarowanie hydrostatyczne, pomiar rozkładu ciśnienia

Summary

One of the known solutions of thrust bearings for heavy machines is a hybrid slide axial bearing composed of a set of bearing pads supported on sets of compression springs. During operation of such a system, a series of failures have been observed. The failures were caused by inappropriate

* AGH University of Science and Technology, Department of Machine Design and Terotechnology, al. Mickiewicza 30, 30-059 Kraków, e-mail: gradkow@agh.edu.pl, jsalwin@agh.edu.pl

parameters of the supporting springs and the appearance of an adverse system of forces acting on the bearing pad.

The paper presents the results of experiments in which pressure distribution in a bearing interspace of a model hydrostatic thrust bearing was measured. The research goal was to verify an earlier formulated quantitative model, describing the conditions at which the mentioned failure occurred. The results of the experiment confirm the legitimacy of the proposed model.

INTRODUCTION

One of the known British firms has developed an original design of water turbine thrust bearing. Significant axial forces are borne by a flanged bush, whose flange mates a sliding ring rested on a set of self-inclining bearing pads. The required self-inclination is assured by settling each bearing pad on a set of high rate compression springs. The bearing is built as a hybrid one. During start-up and run-down, at low rotational speed, required fluid friction conditions are assured by a hydrostatic lubrication system. Each bearing pad has an oil groove, supplied with oil of pressure high enough to generate continuous oil film.

Once the necessary rotational speed is achieved, hydrodynamic lubrication conditions appear. Such bearing system is applied in one of the Polish hydro-electric power stations. The bearing's sliding ring mates sixteen bearing pads supported by sixteen springs each – **Fig. 1**.

In the initial period of turbines operation, a few failures have been recorded, one of those followed by serious consequences. The analysis of the failures' sequence and their outcomes allowed drawing a conclusion, that during the start-up, individual pads self-inclination was incorrect. This led to oil film continuity loss, metallic contact of the mating sliding surfaces, friction parameters change and, in consequence, destabilisation of bearing operation parameters.

The most probable reason for the failure was a dispersion of technical parameters of the supporting springs. This caused non-uniform pads support, which in turn caused uncontrolled inclination of the pads, loaded from above with the hydrostatic oil film. After examination of the springs characteristics, every single of them was assigned strictly specified location. Thanks to this, a required bearing pad supporting forces distribution was obtained. Ever since, the bearings performance was failure-free, which confirms that the conclusions were correct.

a) b)

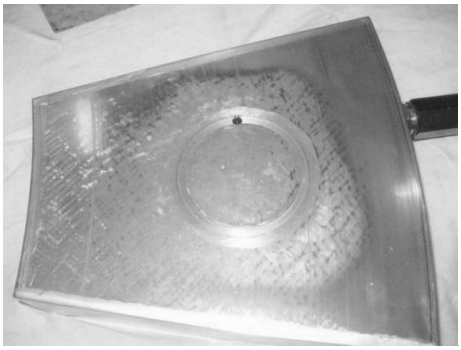

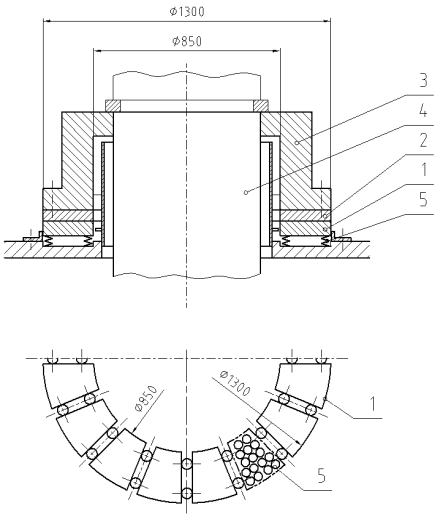

Fig. 1. **Water turbine thrust bearing: a) single bearing pad photo – excessive wear due to failure visible on the surface; b) spring support scheme: 1 – bearing pad, 2 – sliding ring, 3 – flanged bush, 4 – generator shaft, 5 – set of supporting springs**

Rys. 1. Łożysko wzdłużne hydrozespołu: a) fotografia – widoczne zużycie powierzchni wywołane awarią; b) schemat podparcia sprężystego: 1 – segment łożyska, 2 – pierścień ślizgowy, 3 – tuleja kołnierzowa, 4 – wał generatora, 5 – zespół sprężyn podpierających

QUALITATIVE MODEL

The mechanism of loss of stability of the bearing pad in the hydrostatic start-up phase is presented in **Fig. 2**. If all the supporting springs have the same characteristics, the resultant of the spring compression forces should have its application point in the centre of the bearing pad – **Fig. 2a**. Otherwise, the springs share the load unequally. This causes the resultant force application point move. In consequence, the bearing pad tilts, and the geometry of the bearing interspace changes, which in turn makes the oil film pressure distribution change. The oil film acts on the bearing pad with a resultant force, applied in the centre of gravity of an imaginary solid depicting the pressure distribution. As long as the two points lie on a common vertical line, the bearing pad remains stable, although tilted – **Fig. 2b**. If the bearing pad tilt doesn't result in enough large change of the interspace geometry, the two forces F_{oil} and F_{spr} will

create a moment, which will further tilt the bearing pad, until physical contact of the bearing pad's edge and mating surface – **Fig. 2c [L. 1, 2]**.

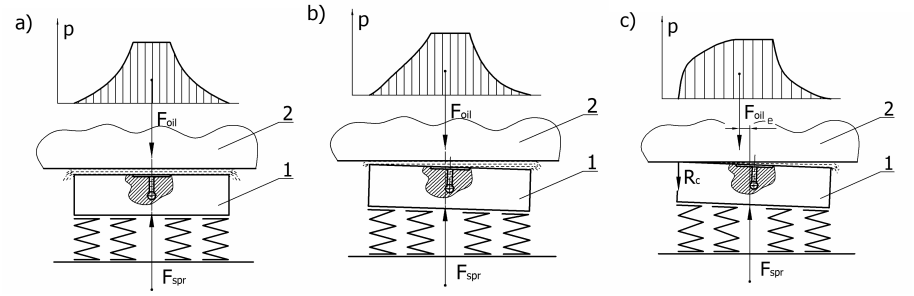

Fig. 2. Behaviour of a bearing pad under the forces of oil film total pressure and springs support resultant: a) resultant spring support force F_{spr} acting in the centre of the bearing pad; b) slightly eccentric resultant causes bearing pad tilt and bearing interspace geometry change; c) significantly eccentric spring support force causes local loss of fluid friction – 1 – bearing pad; 2 – sliding ring

Rys. 2. Zachowanie segmentu łożyska pod wpływem działania sprężyn i hydrostatycznego filmu olejowego: a) wypadkowa siła podparcia sprężynami działa w środku segmentu; b) nieznacznie przesunięta wypadkowa działania siły podparcia, powoduje pochylenie segmentu i zmianę kształtu szczeliny smarnej; c) znacznie przesunięta siła podparcia sprężynami, powoduje lokalną utrata tarcia płynnego – 1 – segment łożyska; 2 – pierścień ślizgowy

RESEARCH STAND

In order to verify the presented quantitative model of fluid friction loss on the bearing pad, a measurement of pressure distribution in the oil film was conducted. The measurement was taken in a hydrostatic oil film generated on an active face of ring-shaped model bearing pad – **Fig. 3**.

It had been assumed, that the ring-shaped face is for the experiment's purpose, a sufficient approximation of a real bearing pad with circular oil groove in the centre. The experiment was performed on a stand, whose essential scheme is presented in **Fig. 4**. The examined bearing pad model (1) rested on a measurement slab (2). Between the mating faces of the model and the slab, a hydrostatic oil film was generated. In the point "p", the measurement slab has a hole, connected to an NPx200 pressure sensor. The measurement slab rests on an additional bearing slab (3), and thanks to the oil film generated between them, has the ability of free movement, so that the point "p" can be placed within 120 mm away from

that point, but only in one direction – the measurement slab has one degree of freedom. The measurement slab location is recorded with a PJx300 linear translation sensor. The data are acquired with an NI USB-6009 data acquisition card. It is also possible to adjust the location of the bearing pad model so, that the load G, simulating the springs support resultant force, can be applied within ±16 mm from the centre of the model. In the corners of the bearing pad model, dial gauges are fixed to measure the oil film thickness.

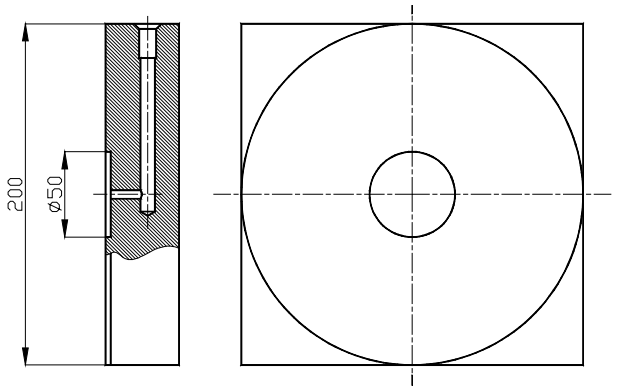

Fig. 3. Sketch of a slide thrust bearing pad model
Rys. 3. Szkic modelu segmentu ślizgowego łożyska wzdłużnego

Pressure distribution measurements were taken at load values G of 40 kN, 60 kN, 80 kN, and 100 kN, and at eccentricity e of the bearing pad model axis and load force between -16 mm, and +16 mm, every 4 mm. Due to mechanical limitations of the stand, during data processing it has been assumed, that the pressure distribution recorded at the same load value and opposite eccentricity values, put together represents pressure distribution along the diameter of the model at the given load and eccentricity.

Additionally, for every pressure distribution, location of the centre of gravity of the area bounded by the pressure distribution plot was calculated, using the trapezoidal rule.

The pressure distribution measurement results were also compared with the isothermal theoretical model of the pressure distribution in a rigid interspace, described by the Reynolds' equation **[L. 3**, **4]**. To calculate the theoretical pressure distribution, finite differences method, described elsewhere **[L. 5**, **6]** was applied.

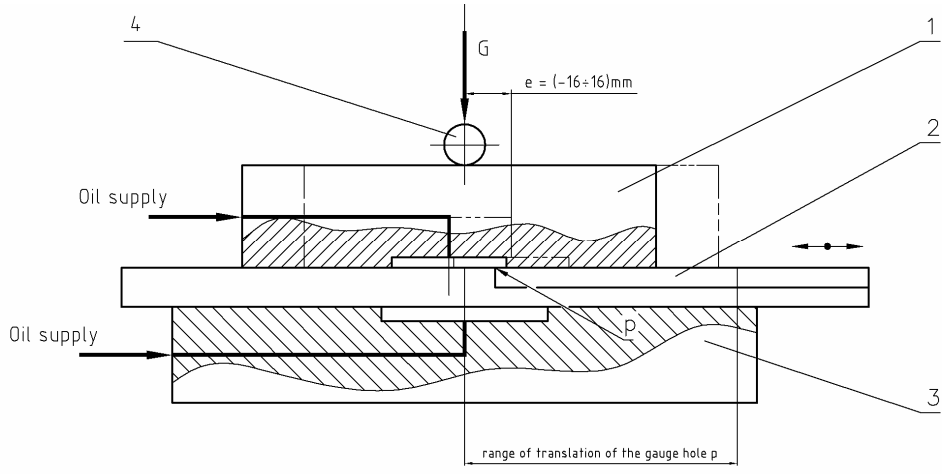

Fig. 4. Essential scheme of the research stand: 1 – examined bearing pad model; 2 – movable measurement slab; 3 – fixed hydrostatic bearing slab; 4 – ball, transferring load. Phantom line represents the range of possible positions of the model during the experiment

Rys. 4. Schemat stanowiska badawczego: 1 – badany segment łożyska (model), 2 – ruchoma płyta pomiarowa; 3 – hydrostatyczna płyta nośna; 4 – kulka przekazująca obciążenie. Linią dwupunktową oznaczono zakres położenia modelu segmentu podczas badań

Table 1. Selected results of measurement of the distance of the bearing pad model corners from the measurement slab face

Tabela 1. Wyniki wybranych pomiarów odległości modelu segmentu łożyska od powierzchni płyty pomiarowej

		Load *G*							
		40 kN		60 kN		80 kN		100 kN	
load eccentricity *e*	-16 mm	-10 μm	-10 μm	20 μm	20 μm	20 μm	20 μm	20 μm	20 μm
		250 μm	260 μm	160 μm	140 μm	140 μm	160 μm	130 μm	130 μm
	-8 mm	20 μm	20 μm	10 μm	20 μm	00 μm	10 μm	00 μm	10 μm
		180 μm	180 μm	140 μm	140 μm	110 μm	120 μm	100 μm	110 μm
	0 mm	100 μm	90 μm	70 μm	80 μm	50 μm	60 μm	50 μm	50 μm
		90 μm	90 μm	80 μm	80 μm	60 μm	60 μm	50 μm	50 μm
	8 mm	160 μm	150 μm	120 μm	130 μm	100 μm	100 μm	90 μm	90 μm
		30 μm	30 μm	20 μm	20 μm	10 μm	20 μm	10 μm	20 μm
	16 mm	200 μm	190 μm	170 μm	160 μm	140 μm	140 μm	130 μm	130 μm
		-20 μm	-20 μm	-20 μm	-30 μm	-20 μm	-30 μm	-20 μm	-30 μm

EXPERIMENT RESULTS

Table 1 presents the results of measurement of the distance of the bearing pad model corners from the measurement slab face (dial gauge readouts). These, indirectly, inform on the oil film thickness, as well as on the mating faces inclination.

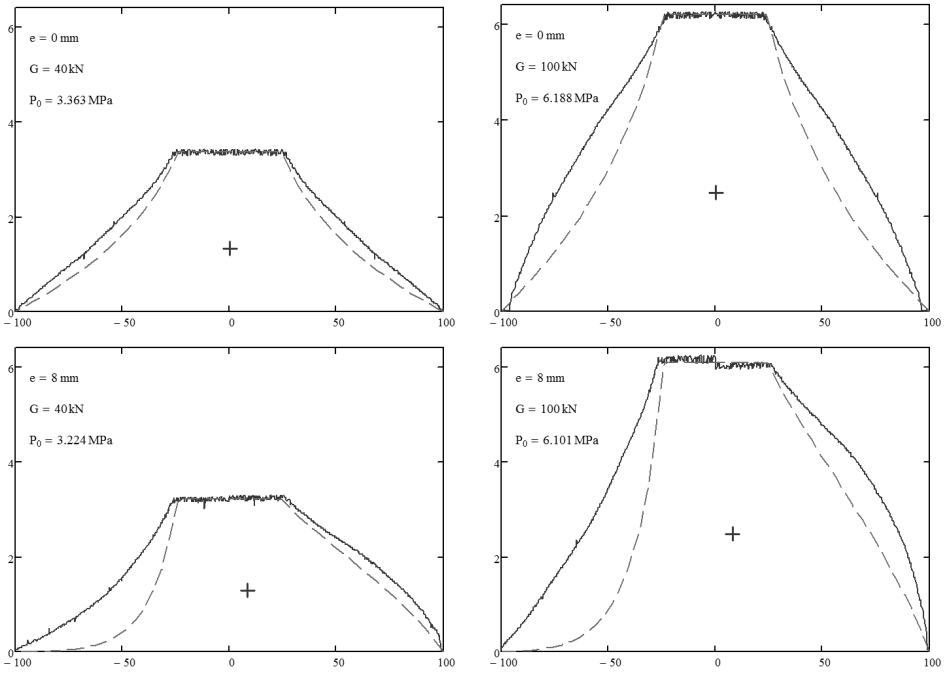

Fig. 5. Selected plots of oil film pressure distribution along the diameter of the model bearing pad; continuous line – measured pressure distribution; dash line – theoretical pressure distribution derived from isothermal model. G – load; e – load eccentricity; P_0 – mean oil groove pressure

Rys. 5. Wybrane rozkłady ciśnienia w filmie olejowym wzdłuż średnicy modelu łożyska stopowego; linia ciągła – rozkład ciśnienia na podstawie pomiarów; linia kreskowa – teoretyczny rozkład ciśnienia wyznaczony z izotermicznego modelu. G – obciążenie modelu; e – ekscentryczność przyłożonego obciążenia; P_0 – uśrednione ciśnienie w komorze smarowej

It is important to mention, that during measurements at extreme eccentricity values (±16 mm), translation of the measurement slab was significantly more difficult, which may indicate local loss of fluid friction. These cases are the ones shaded in **Table 1**. **Fig. 5** presents selected plots

of oil film pressure distribution along the diameter of the model bearing pad. The calculated abscissa coordinates of the centres of gravity, compared with the eccentricity setting are provided in the **Table 2**.

Table 2. Comparison between the set load eccentricity and oil film total pressure application point

Tabela 2. Porównanie ekscentryczności przyłożonego obciążenia z położeniem środka naporu filmu olejowego

		load eccentricity *e*				
		0 mm	4 mm	8 mm	12 mm	16 mm
Load *G*	10 kN	0,046	3,935	7,706	11,339	14,823
	20 kN	-0,102	3,779	7,555	11,153	14,617
	30kN	0,045	3,909	7,686	11,24	14,626
	40kN	-0,281	3,604	7,574	11,36	14,774

RESULTS DISCUSSION

In the middle part of the plots, constant value of the pressure corresponds with the oil groove pressure. Offsets, visible in the very midpoint of some plots are results of inaccuracy in applying the load *G* before measurements – eccentricity change required reducing the load to zero. Despite these irrelevant faults, following conclusions can be drawn:

1. As the eccentricity of the load and the bearing pad axis grows, pressure distribution becomes more asymmetric. The pressure decreases with the growing distance from the oil groove faster on the side, where the interspace widens. This observation is consistent with the conclusions drawn from the previously presented quantitative model.
2. Although for small loads (40 kN), the shape of the plot hardly varies from the theoretical pressure distribution described by a model for a footstep bearing **[L. 7]**, it is clear that for greater loads the difference is more significant. In the proximity of the oil groove, the pressure decreases slower, than it should according to the theoretical model, later the decrease rate is faster than the mathematical model describes. Most probably it is caused by deflection of either the bearing pad model, or the measurement slab under the acting pressure. Where the pressure is high, that is near the oil groove, greater deflection

causes interspace thickness increase and less bounded oil flow. This explains slower pressure decrease in that area. As the distance from the oil groove increases, the deflection decreases, as well as the oil film thickness. The oil, flowing through a tapering interspace experiences increasing resistance, which consumes its energy.

3. Location of the numerically calculated centre of gravity of each plot insignificantly deviates from the set eccentricity of the load. This indicates the situation, when support resultant and total pressure force act along a common line (**Fig. 2a** and **2b**). For eccentricity set to 16 mm the centre of gravity is about 2 mm closer to the centre of the bearing pad, than the line of direction of the load *G*. This represents the situation presented in **Fig. 2c**, where the support resultant force, and total pressure force create a moment, countered by mechanical reaction force on the edge of the bearing pad.

CONCLUSIONS

The experiments carried out confirm the quantitative model of loss of oil film continuity on the active face of an axial bearing pad. This refers both to the pressure distribution and the system of forces acting on the bearing pad at hydrostatic stage of performance. Simplification of the bearing pad, by modelling it with a ring-shaped face allowed clear observation of results.

Certain inconsistency has been observed between the measurement results and the mathematical description of pressure distribution in the bearing interspace. Increasing deviations at larger loads suggest, that one of the factors, neglected in mathematical model is elastic deflection of parts. Most likely, the experiment was mainly affected by relatively small rigidity of the measurement slab, loaded not only with the researched oil film from above, but also the supporting hydrostatic film from below. This supposition is confirmed by negative recorded values of distance of the model corners from the slab surface.

REFERENCES

1. Salwiński J., Rupeta W., Grądkowski P.: Nekotorye aspekty modernizacii karmana v segmentnom gidrostaticeskom podsipnike gidrogeneratora – international conference „Problemy sovremennoj mehaniki" Almaty, Kazahstan 2006.

2. Salwiński J., Grądkowski P.: Modelowanie rozkładu ciśnienia w filmie olejowym asymetrycznie obciążonego segmentu hydrostatycznego łożyska wzdłużnego – Zagadnienia Eksploatacji Maszyn vol. 42/2007.
3. Kiciński J.: Teoria i badania hydrodynamicznych poprzecznych łożysk ślizgowych. Wydawnictwo PAN Wrocław, Warszawa, Kraków 1994.
4. Świderski W.: Właściwości adiabatycznego filmu olejowego w poprzecznych łożyskach ślizgowych. Zeszyty naukowe Politechniki Łódzkiej nr 706. Rozprawy naukowe, Z. 208. Łódź 1995.
5. Evans G., Blackledge J., Yardley P. Numerical Methods for Partial Differential Equations. Springer Verlag London Ltd 2001.
6. Salwiński J., Grądkowski P.: Komputerowe modelowanie stanu równowagi segmentu łożyska wzdłużnego wspartego na zespole elementów sprężystych. XVI Konferencja nt. „Metody i środki projektowania wspomaganego komputerowo" Krasiczyn, październik 2009.
7. Fuller D.D.: Theory and Practice of Lubrication for Engineers. New York, John Wiley & Sons, Inc., 1956.

Recenzent:
Stanisław PYTKO

Streszczenie

Jednym ze stosowanych rozwiązań łożyskowania wzdłużnego ciężkich maszyn jest łożyskowanie w hybrydowym ślizgowym łożysku wzdłużnym, złożonym z segmentów wspartych na elementach sprężystych. W trakcie eksploatacji takiego układu zaobserwowano szereg awarii, polegających na niezamierzonym metalicznym kontakcie powierzchni ślizgowych. Awarie były spowodowane niewłaściwymi parametrami sprężyn wspierających segmenty i wystąpieniem niekorzystnego układu sił działających na segmenty łożyska.

W pracy zaprezentowano wyniki badań stanowiskowych rozkładu ciśnienia w szczelinie smarnej modelu hydrostatycznego łożyska wzdłużnego. Badania służyły weryfikacji, sformułowanego wcześniej, modelu jakościowego opisującego warunki wystąpienia opisanej awarii. Wyniki badań potwierdzają słuszność zaproponowanego modelu.